

Compressed Real Numbers for AI: a case-study using a RISC-V CPU

FEDERICO ROSSI¹, MARCO COCOCCIONI¹, (Senior Member, IEEE), ROGER FERRER IBÁÑEZ², JESÚS LABARTA², FILIPPO MANTOVANI², MARC CASAS², EMANUELE RUFFALDI³, (Senior Member, IEEE) and SERGIO SAPONARA¹, (Senior Member, IEEE),

¹Department of Information Engineering, University of Pisa, Pisa, Italy (e-mail: federico.rossi@ing.unipi.it, marco.cococcioni, sergio.saponara@unipi.it)

²Barcelona Supercomputing Center, 08034 Barcelona, Spain, (e-mail: {roger.ferrer, jesus.labarta, filippo.mantovani, marc.casas}@bsc.es)

³MMI spa, (e-mail: emanuele.ruffaldi@mmimicro.com)

Corresponding author: Federico Rossi (e-mail: federico.rossi@ing.unipi.it).

Work partially supported by the following H2020 projects: EPI SGA2 (grant agreement 101036168), EuPilot (grant agreement 101034126) and TextaRossa (grant agreement 956831).

• **ABSTRACT** As recently demonstrated, Deep Neural Networks (DNN), usually trained using single precision IEEE 754 floating point numbers (*binary32*), can also work using lower precision. Therefore, 16-bit and 8-bit compressed format have attracted considerable attention. In this paper, we focused on two families of formats that have already achieved interesting results in compressing *binary32* numbers in machine learning applications, without sensible degradation of the accuracy: *bfloat* and *posit*. Even if 16-bit and 8-bit *bfloat/posit* are routinely used for reducing the storage of the weights/biases of trained DNNs, the inference still often happens on the 32-bit FPU of the CPU (especially if GPUs are not available). In this paper we propose a way to decompress a tensor of *bfloat/posit*s just before computations, i.e., after the compressed operands have been loaded within the vector registers of a vector capable CPU, in order to save bandwidth usage and increase cache efficiency. Finally, we show the architectural parameters and considerations under which this solution is advantageous with respect to the uncompressed one.

• **INDEX TERMS** RISC-V processors, instruction set architecture extension, vectorized operations, Deep Neural Networks, Hardware-Software Co-Design, *posit* arithmetic.

I. INTRODUCTION

In the last years the RISC-V open-source architecture has been put under the spotlight [1]–[3]. Thanks to its open nature and absence of royalties, it is making its way among the big microprocessor companies like Intel, AMD, and Arm. Moreover, several hardware and software companies are contributing to the initiative, other than public and private universities around the globe.

Thanks to its modularity, the RISC-V architecture offers multiple extensions for the instruction set architecture (ISA). Furthermore, it provides the possibility to customise and expand the base ISA. Among the interesting ISA extensions developed for this new architecture, the vector extension is one of the most advanced and promising for high-performance computing (HPC) and machine learning. In particular, this instruction set extension complements pre-existing architectures like SSE/AVX (Streaming SIMD Extension/Advanced Vector eXtension) by Intel, and SVE (Scalable Vector Extension) by Arm.

All these extensions also aim to overcome the absence of GPUs/TPUs (Graphics/Tensor Processing Units) in several hardware ecosystem, while promoting a coherent programming paradigm across the architectures. Moreover, thanks to the vector length agnostic approach taken by Arm and RISC-V, the portability of applications can skyrocket in the same architecture environment, without the need to adapt each program for different configurations of the same architecture.

In combination with these new advancements in machine learning and HPC applications, several new optimisations in information representation have been proposed by both industry and academia. In particular, the focus has shifted to reducing computation and space complexity in handling floating-point computations, which are pervasive in the machine learning world. Among the others, some deserve important credits: Intel with Flexpoint [4, 5], Google with *bfloat16* [6], IBM with *DLFloat16* [7], Facebook AI with logarithmic numbers [8], and Tesla with Configurable Floats [9].

In this paper, we mainly focus on Google bfloat and on another, very promising, number system: the posit™ format. Posit numbers have been proposed by J. L. Gustafson [10] and proven to match the accuracy obtained when using 32-bit floating point numbers (i.e., the so called *binary32*, according to the IEEE 754/2019 standard) with that achieved by 16-bit posits [11]–[17]. In the meantime, several researchers have pushed towards hardware implementations of this new format, showing how it can be interesting in terms of power consumption and on-chip area utilisation [18, 19].

Our goal in this work is to combine both the two emerging approaches (a vectorized RISC-V processor and the arithmetic compression), where a smaller format is used as a compressed storage format to be used in a big length (up to 16384-bit) vectorized CPU. The combination between a highly compressed format (down to 16-bits, so up to a factor 2 with respect to a standard *binary32* representation for weights and activations) and a large vector register environment can be particularly interesting when the architecture allows to fit entire matrices or vectors inside a single vector register. Moving 16-bit operands instead of 32-bit operands improves the memory/CPU data transfer bandwidth, has a positive impact on all the caches, and allows to put more operands within the vectorized environment at the same time.

Furthermore, in the paper, we push towards testing the capabilities of this approach in a hardware platform, exploiting an advanced model of a real RISC-V vector processor. We use the Vehave emulator and MUlti-level Simulation Approach (MUSA) simulator to evaluate the impact of our approach.

A. CONTRIBUTIONS OF THIS WORK

In this paper we envision the use of compressed numerical formats to store and transfer data, to be used in the RISC-V vector environment; the work is aimed at extending what have been done in [20]. More precisely, in the present extension we address two topics not addressed before: the use of alternative numerical formats for DNN *data compression* (weights and activations) on common operations when training DNNs (i.e., the matrix-matrix multiplication and convolution), for providing feedbacks to RISC-V Register Transfer Level (RTL) designers. More precisely, we want to assess under which conditions the decompression ("widening") of the weights/activations can be delayed at the latest, i.e., only once the data has been loaded within the CPU, and by using vectorized instructions for decompression/compression. Similarly to [20], even in this work we assume to not have GPUs/TPUs, a situation which is not uncommon. The presence of GPUs/TPUs will be addressed in a future study.

B. ORGANISATION OF THE PAPER

In Section II we present the RISC-V vector extension and we describe on the emulation and simulation ecosystem, including an overview of the tools used in the subsequent sections.

In Section III we present the bfloat and the posit formats, the two compressed format for DNN weights/biases considered in this work.

In Section IV we present the proposed approach, namely, the in-register compression and decompression method to deal with 16-bit real number formats.

In Section V we present the obtained results on a GEMM kernel with different matrix sizes and vector register lengths, evaluating the impact of the instruction set architecture on the overall latency.

Finally, we draw conclusions in section VI.

II. THE RISC-V PROCESSOR AND THE "V" EXTENSION

The key aspect of the RISC-V Instruction Set Architecture (ISA) is its modularity [1]. Indeed, we can build whichever combination of RISC-V ISA subsets to match application requirements.

In this paper we will focus on the vector extension, namely, "V" extension. This extension aims to provide a Single Instruction Multiple Data (SIMD) unit to the RISC-V processor architecture.

The current lack of hardware implementations of the RISC-V vector extensions can be mitigated by using a set of tools that runs on top of a basic RISC-V processor, either physical or emulated through virtualisation software such as QEMU (Quick EMULATOR, <https://www.qemu.org/>). In this paper we will use the RISC-V 64-bit (RV64GC) processor Sifive U74-MC. Hereafter we will describe the set of tools used to emulate and analyze the behaviour of vectorize programs on a RISC-V vector capable processor (using the 1.0 revision of the vector extension).

A. THE VEHAVE EMULATOR

Vehave is a user-space emulator for the V-extension of the RISC-V ISA that runs on RISC-V Linux. It allows a functional verification of a program that uses V-extension instructions or a code generator, such as a compiler, that emits V-extension instructions. The goal is to help porting applications that run in a well-known environment, such as Linux. Only a compiler or code generator that can emit V-extension instructions is needed.

Vehave emulates instructions by intercepting the illegal instruction exception that a CPU emits when it encounters an unknown/invalid instruction. Once an illegal instruction is found, Vehave decodes it and if it is a valid V-extension instruction it emulates it, otherwise an error is propagated back. The program resumes once the emulation of the vector instruction is complete. Figure 1

provides a simplified graphical representation of the emulation dynamic of Vehave.

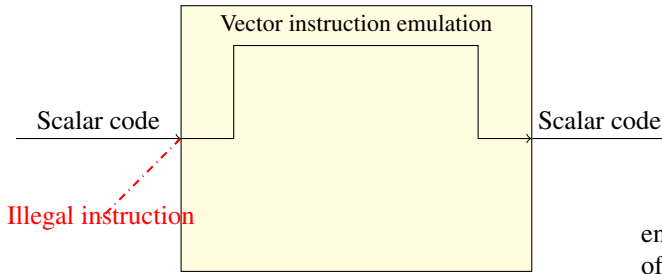


FIGURE 1: Graphical representation of the Vehave emulation scope (yellow).

Vehave relies on the LLVM libraries of the compiler which already supports the V-extension for the process of decoding the instructions. The output of Vehave is collected in a `.trace` file which stores in plain text extensive details about each vector instruction emulated and some quantitative figure of the scalar code executed before each vector instruction.

B. THE PARAVR TRACE ANALYZER

The `.trace` file generated by Vehave are parsed and converted to `.prv` format which can be visualised with Paraver [21]. Paraver is a visualisation tool originally developed to allow a qualitative global perception of the behavior of complex parallel HPC applications previously run acquiring traces on a cluster of compute nodes. Even if the interposition library to gather the information stored in the trace is different in an HPC cluster and in Vehave, the navigation features of Paraver are flexible enough to allow studying almost any timestamped series of data converted to the `.prv` format [22].

Paraver offers a graphical interface to analyze several aspects of the vector program execution. The two main visualization configurations are timelines and histograms (or tables). Timelines allow visualizing (with different colors) the data encoded in the trace such as: the value of the program counter, the content of the registers used by each vector instruction, and the addresses of memory accesses. Histograms are used to quantitatively inspect the content of the traces and allow to easily collect the number and type of vector instructions as well as the register utilization.

C. THE MUSA TRACE ENRICHER

While Vehave has full visibility on vector instructions and their scope in the code, it does not allow to collect performance information. The vehave emulator produces a trace of dynamic instructions without any performance estimation. The MUSA trace enricher incorporates a timing model capability in the Vehave emulation infrastructure that uses the initial Paraver trace to drive a micro-architecture simulation. From this simulation, it



FIGURE 2: Illustration of a bfloat16 number.

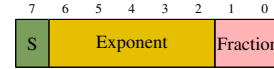


FIGURE 3: Illustration of a bfloat8 number.

enriches the trace by adding precise information in terms of instruction latency, memory hierarchy level where accesses are served, or commit cycle time. The MUSA timing model keeps all information present in the first Paraver trace unaltered and adds additional timing and performance data. On top of the data stored in the trace, MUSA considers different architectural abstractions to simulate fundamental aspects like memory hierarchy, instruction dependencies, or out-of-order pipeline.

Using textual configuration files we can instruct MUSA to simulate several architecture configurations such as instruction latency for all the vector instructions, number and size of cache levels, memory access latency and size, number of re-order buffer entries (ROB size) and other similar information about the underlying architecture.

The output of the MUSA trace enricher can be analysed using Paraver as well, thoroughly visualising all the architecture behaviour during the execution of a vector program coupled with timing information. This way we are able to estimate both *i*) the performance of the vector implementation of our algorithms, and *ii*) the effect of architectural changes on our code.

III. COMPRESSED FORMATS

In this section we review the two compressed formats investigated in this study: bfloat and posit (while bfloat is deeply investigated in this work, posit is only theoretically evaluated at the end, comparing its complexity to the bfloat format). These two formats were demonstrated to be able to replace binary32 format in deep learning tasks with very little degradation in accuracy, while reducing the memory footprint by a factor 2 [17].

A. THE BFLOAT FORMAT

The bfloat16 format [6] is a 16-bit fixed-size format. It has 3 fields as shown hereafter:

- Sign field: 1-bit
- Exponent field: 8-bit (same as the binary32 format)
- Fraction: 7-bit

The format relaxes several IEEE binary32 standard features to allow low-cost hardware implementations. In particular: (i) subnormals are clamped to 0; (ii) only one rounding mode is supported; (iii) NaN are not propagated; (iv) no IEEE exception flags.

The format can particularly fit to neural networks as an easy replacement for IEEE binary32 numbers. The main advantages of this format are: (i) drop-in replacement for IEEE binary32 with comparable neural network accuracy; (ii) smaller footprint, hence increased throughput with regards to IEEE binary32 format; (iii) conversion between IEEE binary32 number and bfloat16 can be performed with a right-shift or a right zero padding, respectively.

The bfloat family also includes a 8-bit format, namely bfloat8. The format is a fixed-size one, with 3 fields as shown hereafter:

- Sign field: 1-bit
- Exponent field: 5-bit
- Fraction field: 2-bit

As we can see from the format, the bfloat8 cannot be obtained by a simple bit-shift of the 16-bit counterpart. Instead, it can be obtained with a right shift of a binary16 (a.k.a floating point 16, fp16) number by 8 positions. This means that, in an architecture with hardware support for binary16 numbers, we can exploit this property to easily convert between binary16 and bfloat8 numbers.

B. THE POSIT FORMAT

The posit format [10, 23]–[25] is a fixed length format, where the total length and exponent length can be configured. It can have a maximum of 4 fields as in Figure 4. The fields in a posit number are:

- Sign field: 1 bit;
- Regime field: variable length, composed by a string of bits equal to 1 or 0 ended, respectively by a 0 or 1 bit;
- Exponent field: at most $esbits$ bits (it can even be absent);
- Fraction field: variable length fractional part of the significand (it can even be absent too).

Given a *posit* $\langle nbits, esbits \rangle$, represented in 2's complement signed integer X and let e and f be exponent and fraction values, the real number r represented by X encoding is:

$$r = \begin{cases} 0, & \text{if } X = 0 \\ \text{NaN}, & \text{if } X = -2^{(nbits-1)} \\ \text{sign}(X) \cdot used^k \cdot 2^e \cdot (1+f), & \text{otherwise.} \end{cases} \quad (\text{Not a Real})$$

The value *used* is $used = 2^{esbits}$ and the number k is the value of the regime. The value k is strictly

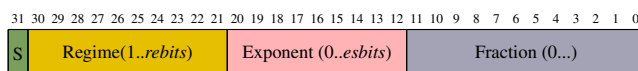


FIGURE 4: Illustration of a $\text{posit}\langle 32, 9 \rangle$ data type. Both the exponent and the fraction field can be absent, for specific configurations having a regime field particularly lengthy.

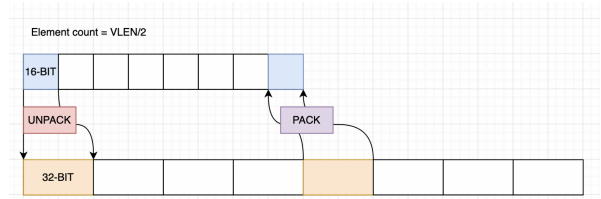


FIGURE 5: Process of unpacking and packing a vector of a generic compressed format directly inside a VPU register.

related to the regime length l and bitstring (b is the bit that composes the string of identical bits, e.g. in 00001 $b = 0$). If $b = 0$ the k is negative, otherwise the k is positive:

$$k = \begin{cases} -l, & \text{if } b = 0 \\ l - 1, & \text{otherwise.} \end{cases}$$

In [26] we brought this kind of implementation into the vectorization field, implementing several posit operations such as ELU and Tanh exploiting the already existent vector integer operations in the RISC-V vector environment.

IV. IN-REGISTER COMPRESSION AND DECOMPRESSION

The core idea of the approach we propose in this paper is the decompression of compressed numbers to be performed inside the RISC-V vector registers exploiting vector instructions. In this way we aim to reduce the memory transfer to the vector registers; indeed, instead of loading N elements of 32-bit, we will load the same N elements but compressed on 16-bit.

In particular, as shown in Figure 5, when we need to decompress (or unpack) a vector filled with bfloat16 elements we start reasoning about the vector register length.

Given that we need to expand a 16-bit format inside a 32-bit one, when filling the vector register we fill just half of the vector register. Then we can expand each vector element using the RISC-V vector instructions.

Same approach is considered when we need to compress the binary32 format back to the original 16-bit one.

While this approach can be generalized to any compressed 16-bit format, it may perform very differently when applied to different low precision format.

In particular, the unpack and pack phases may involve several different instructions to perform the necessary bit manipulations for the type conversions.

While a $\text{Posit}\langle 16, 2 \rangle$ can have a very little drop in accuracy when converted from binary32, the conversion involves the use of several bit manipulations to be completed. This means that the un/pack phases can potentially take a lot of computing cycles. On the other hand, if we could have specific hardware instruction for

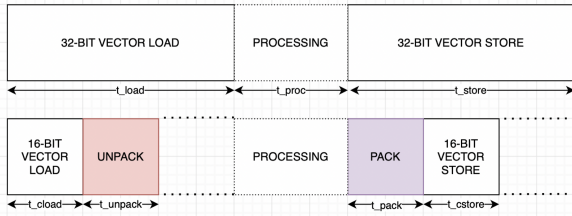


FIGURE 6: Timeline of a generic linear algebra algorithm that employs in-register decompression and compression.

vectorized posit to float (and viceversa) conversions, we could sensibly reduce the latency of said operations.

There are other formats, such as bfloat16, that are designed to allow seamless conversion with the binary32 format.

In particular the two phases involve following instructions:

- binary32 \rightarrow bfloat16: logic right shift of 16 digits
- bfloat16 \rightarrow binary32: left shift of 16 digits with 0 padding on the least significant bits

Since the two steps have an inherent cost for the conversion we need to take into account the computation effort spent on and decompression and compression.

In Figure 6 we show our approach in detail. Suppose we need to process some data with a given algorithm, whose processing time will be t_{proc} on a given architecture. If we imagine to load the N elements to be processed using a 32-bit representation we will need (on average) t_{load} .

On the other hand we can imagine that, on average the load for the same number of elements, represented on 16-bit, will need t_{cload} , where $t_{cload} \sim t_{load}/2$.

In the second case we will also need to pack and unpack the compressed format so we will add a t_{pack} and t_{unpack} to the timeline.

At this point we can compare the two timelines and write the following requirements:

$$t_{cload} + t_{unpack} < t_{load} \quad (1)$$

$$t_{pack} + t_{cstore} < t_{store} \quad (2)$$

If both these requirements hold, we can obtain an advantage on computation time using this approach.

A further advantage we can theoretically see with our approach is the possibility to exploit instruction overlapping offered by an out-of-order vector processor.

In particular, consider that we are dealing with successive independent computations of separate pieces of data. We can imagine that a 16-bit vector load for the $(n + 1)$ -th piece of data can be performed while the unpacking of the n -th piece of data.

As shown in Figure 7, the same idea can be applied to the different independent parts of the overall process.

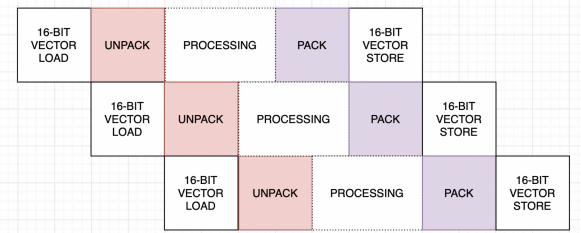


FIGURE 7: Possibility of interleaving the sequence of instructions seen in Figure 6.

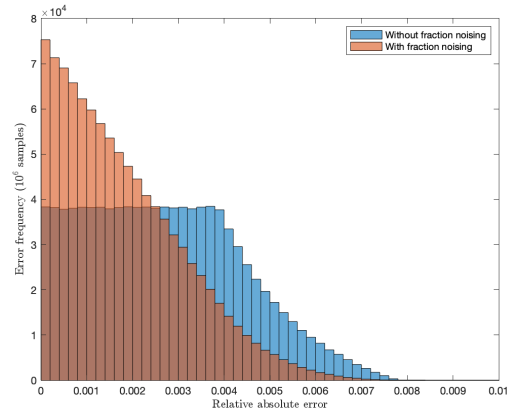


FIGURE 8: Relative absolute error density distribution in conversion between IEEE 32-bit floating points and 16-bit bfloats, computed on 10^6 random samples.

While the same concept would be the same even in the 32-bit load case, note that having smaller parts of independent processing phases on data helps the interleaving of the instructions. Indeed, given that a 32-bit load takes twice as long than the 16-bit counterpart, the interleaving will start with an increased latency.

In terms of accuracy, since every operation is executed using 32-bit floating point arithmetic, the loss in precision only happens when converting from 32-bit float into the 16-bit format. Figure 8 shows the density distribution of the absolute relative error that happens during conversion between 16-bit bfloats and 32-bit IEEE floating points. The blue curve in Figure 8 shows the error distribution when converting from FP32 from/to BF16 ignoring the least 16 significant bits of FP32. The red curve in Figure 8 shows the same distribution after we have applied a noise to the FP32 fraction when converting from BF16 to FP32: instead of padding 16 zeroes to the right of the BF16 we simply reproduce the 16 most significant bits into the 16 least significant bits. As reported in the two plots, this technique sensibly reduce the relative error during the conversion forth and back.

V. METHODOLOGY AND EXPERIMENTAL RESULTS

In this section we aim to demonstrate in which conditions our approach can outperform the traditional one (i.e. whether a 16-bit compressed load & decompression outperforms the 32-bit uncompressed load). We focus on the number of committed instructions, computing cycles and average instruction latency, provided by the Vehave simulation tool. We tested the following algorithms, equipped with decompression/compression approach, on a matrix-matrix multiplication kernel.

Listing 1 shows an example of the proposed approach for the GEMM case. We started from a generic GEMM algorithm and modified it to directly load bunch of 16-bit compressed matrix lines and then we decompress them in-register, before computing the multiplication.

In particular, Listing 2 and 3 show the actual implementation of decompression and compression techniques.

A. METHODOLOGY

In order to evaluate the goodness of our approach we compare the in-register de/compression approach to a generic kernel that does not employ compression. As a recap:

- Compressed approach: images/weights are stored as bfloat16 numbers. During kernel execution, data is loaded in bunch of 16-bit elements inside the VPU registers and then it is decompressed to binary32 expanding it to occupy the remaining space inside vector registers. Computations are carried out using binary32 vector instructions already implemented by the RISC-V vector extension.
- Uncompressed approach: images/weights are stored as binary32 numbers. Everything is loaded uncompressed and computation is carried out on binary32 data.

In both cases we monitor the number of computing cycles spent to carry out the kernel several times.

B. EXPERIMENTAL RESULTS

We tested the approach described in the previous sections to the GEMM algorithm. In detail, we run the binaries inside the Vehave simulator, running on a RISC-V virtual machine. Then, we captured the trace output of our binaries running on the Vehave simulator and we fed them to the MUSA simulator. We used 128×128 , 256×256 , 512×512 sizes for the matrices in the experiments. Furthermore, we varied the length of the vector registers in 4096, 8192, 16384 bits to assess the impact of this parameter on the proposed approach. We firstly measured the number of committed vector instructions and then, exploiting a RISC-V processor timing model we obtained the average latency for each committed instruction, so that we could assess the latency impact of our approach in the different configurations.

Figure 9 reports the number of committed instructions required to complete the different algorithm, both with compressed and un-compressed approach. We used a logarithmic scale for the y-axis to fit both frequent and less frequent instructions inside the same plot. From the comparison we can see that the compressed approach has additional instructions related to the compression and decompression phases. In particular, the new instructions are:

- `vnsrl`: logical shift right with narrowing from 32-bit to 16-bit. This instruction is used to directly compress a 32-bit binary32 vector into a 16-bit bfloat16 one, discarding the least 16 significant bits of the fractional part.
- `vwmul`: this instruction has the opposite effect of the previous one: this is used to directly decompress a 16-bit bfloat16 vector into a 32-bit binary32 one, by padding 16 zeroes to the right of the bfloat number (actually multiplying by 2^{16}).
- `vsetvli`: this instruction is automatically inserted by the compiler whenever we change from handling 32-bit elements to 16-bit ones and vice-versa. This instruction is completely unrelated to the proposed approach and it is specific of the vector architecture being used.

Another difference that emerges from the comparison is that the compressed approach has the same amount of load and stores but carried out on 16-bit elements, whereas the uncompressed approach resorts to load and store uncompressed elements on 32-bits.

Since the number of instructions cannot solely measure the impact of this difference we also simulated the program using the Tasksim RISC-V simulator. For this task we only considered the largest workload (i.e. 512×512 GEMM) with 16Kbits vector registers. The simulator embeds a timing model of a RISC-V processor and uses the trace files output by Vehave to produce detailed statistics and in particular, the overall number of computing cycles elapsed to complete program execution. This metric is used to assess the improvement of the compressed approach (cycles_c) over the non-compressed one (cycles_u). We define the improvement metric as follows.

$$\text{improvement} = 100 \times \left(1 - \frac{\text{cycles}_c}{\text{cycles}_u} \right) \quad (3)$$

The improvement metric is impacted by a series of parameter of the simulator:

- L1 data cache size and latency
- Memory bandwidth and latency
- Latency of the overhead instructions used for compression and decompression (i.e. `vnsrl`, `vwmulu`).

Firstly, we considered L1 cache size and memory bandwidth fixing memory latency at 60ns and cache latency at 20ns. Figure 10 shows the variation of the

Listing 1: GEMM algorithm with in-register de/compression.

```

void gemm_16(...) {
    const unsigned long int rvcntw = __builtin_epi_vsetvmax(__epi_e32, __epi_m1);
    for (unsigned long int i = 0; i < M; ++i)

        for (long unsigned int j = 0; j < N; j += rvcntw) {

            unsigned long int all_gvl = __builtin_epi_vsetvmax(__epi_e32, __epi_m1);
            __epi_4xf32 accum = __builtin_epi_vfmv_v_f_4xf32(0.0f, all_gvl);
            unsigned long int gvl = __builtin_epi_vsetvl(N-j, __epi_e32, __epi_m1);
            #pragma clang loop unroll_count(32)
            for (uint32_t k = 0; k < K; ++k) {

                auto A_i_k = ...;
                auto B_k_j = bfloat16_unpack(&B[k * N + j], gvl);

                accum = __builtin_epi_vfmacc_4xf32(accum, A_i_k, B_k_j, gvl);

            }

            bfloat16_pack(&C[i * N + j], accum, gvl);

        }
}

```

Listing 2: Vectorized bfloat16 → binary32 load

```

inline __epi_4xf32 bfloat16_unpack(const signed short int *data,
                                   unsigned long grantedLength) {
    // Expand 16-bit integer StorageType to 32-bit integer
    // 1. Load vector
    __epi_4x16 data_v = __builtin_epi_vload_4x16(data, grantedLength);

    // 2. Expand using widening
    __epi_4x32 wdata_v = __builtin_epi_vwadd_4x32(
        data_v, __builtin_epi_vmv_v_x_4x16(0, grantedLength), grantedLength);

    // Conversion operations
    __epi_4x32 res_v = __builtin_epi_vsl1_4x32(
        wdata_v, __builtin_epi_vmv_v_x_4x32(16, grantedLength), grantedLength);

    // Reinterpret 32-bit integers as vector wide type
    return (__epi_4xf32)res_v;
}

```

TABLE 1: Improvement of the compression approach with low-end and high-end memory bandwidth and cache sizes.

Cache size	Memory bandwidth	
	1GB/s	100GB/s
512KB	97.3%	77.3%
1MB	59.3%	20.4%
2.5MB	6.8%	4.1%

improvement when using the compression approach when changing the memory bandwidth and cache size. As reported, the peak improvement is associated with a cache size of 512Kb. In particular, with this cache size, the improvement spans from 77% with a 100GB/s bandwidth up to 97% with a 1GB/s bandwidth. Table 1 reports the details of the improvement with selected cache and bandwidth configurations.

Secondly, we fixed a reasonable cache size of 1MB

and then varied the L1 cache latency, memory latency and bandwidth to analyse their impact. Figure 11 shows the variation of the improvement between the compressed and un-compressed approach. As expected, the lower the bandwidth the higher the benefits of compressing data to be transferred. Moreover, the higher the memory latency, the higher the impact of the compression in terms of improvement. Furthermore, the workload considered does not benefit from increasing the bandwidth over 50GB/s with these configurations.

Finally, we considered the latency of the instructions executed for the compression and decompression. We selected beforehand the following configurations for the architecture:

- Memory bandwidth: [10, 50, 100]GB/s
- Cache latency: 15ns
- Memory latency: [50, 70, 90, 110, 130, 150]ns
- Cache sizes: [512KB, 1MB, 2.5MB]

Listing 3: Vectorized binary32 → bfloat16 store

```

inline void bfloat16_pack(signed short int *dst, __epi_4xf32 data,
                        unsigned long grantedLength) {
    // Reinterpret 32-bit floats into 32-bit integers
    __epi_4xi32 idata_v = (__epi_4xi32)data;

    // Conversion operations + narrowing operation
    __epi_4xi16 res_v = __builtin_epi_vnsrl_4xi16(
        idata_v, __builtin_epi_vmv_v_x_4xi16(16, grantedLength), grantedLength);

    // Store back the value in memory
    __builtin_epi_vstore_4xi16(dst, res_v, grantedLength);
}
    
```

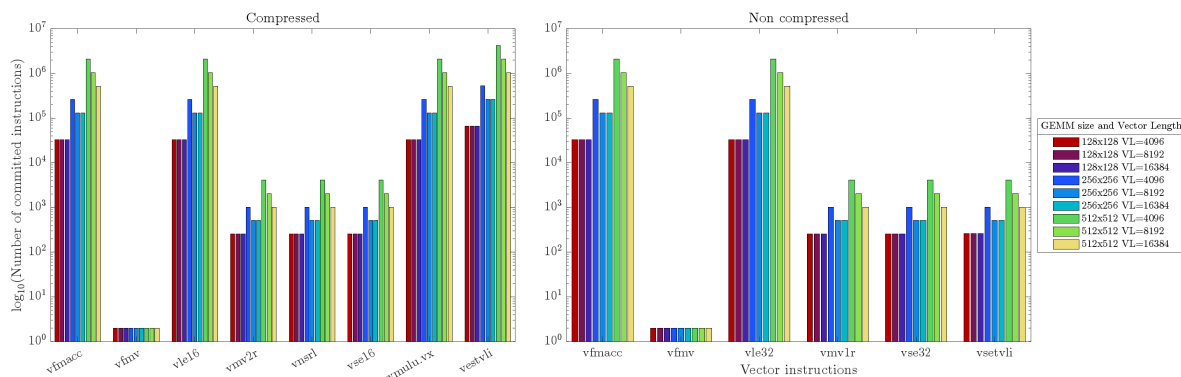


FIGURE 9: Number and type of vector instructions for a GEMM execution with the two approaches.

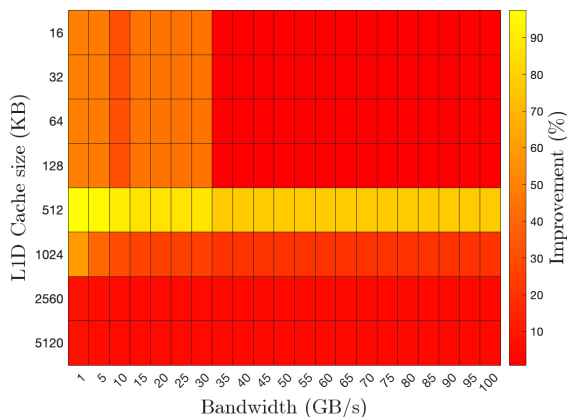


FIGURE 10: Improvement using the compression approach when varying the memory bandwidth and L1 cache size.

- Instruction latency: [1, 10, 20, 30, 40, 50] cycles.

Figure 12 shows the impact of the different architecture parameters on the improvement when using the compression approach. As expected and theorised in the previous section, the latency of compression and decompression instruction has a great impact on the improvement metric. In particular, an instruction latency over 20ns corresponds to a sharp drop in the improvement,

even nullifying it for bigger caches and bandwidths (as we can see in the third column of Figure 12). Analysing this behaviour is fundamental to understand the requirements of a compressed real number representation to be used with this approach. Indeed, the seamless conversion between bfloat16 and fp32 can be obtained with the cost of a single ALU operation. Concluding, the information gathered and represented in Figure 12 can serve as a comparison with other compressed real number formats such as posits in terms of the achievable improvement when used to compress memory data transfers.

C. THE IMPACT OF POSIT DE/COMPRESSION

Without modifying the existing instruction set architecture, the conversion between a 16-bit posit and a 32-bit floating point has a much higher cost in terms of number of instruction and therefore in terms of overall latency. However, if we managed to have a single instruction that was able to perform this operation (with a dedicated hardware unit) with a latency that is compatible with the ones shown in Figure 12 we could employ also 8 or 16-bit posits for this task.

VI. CONCLUSIONS

In this paper, we have demonstrated the implementation of a GEMM kernel using compressed real number formats on a RISC-V vector architecture. The significance of this kernel lies in its potential to serve as a demonstra-

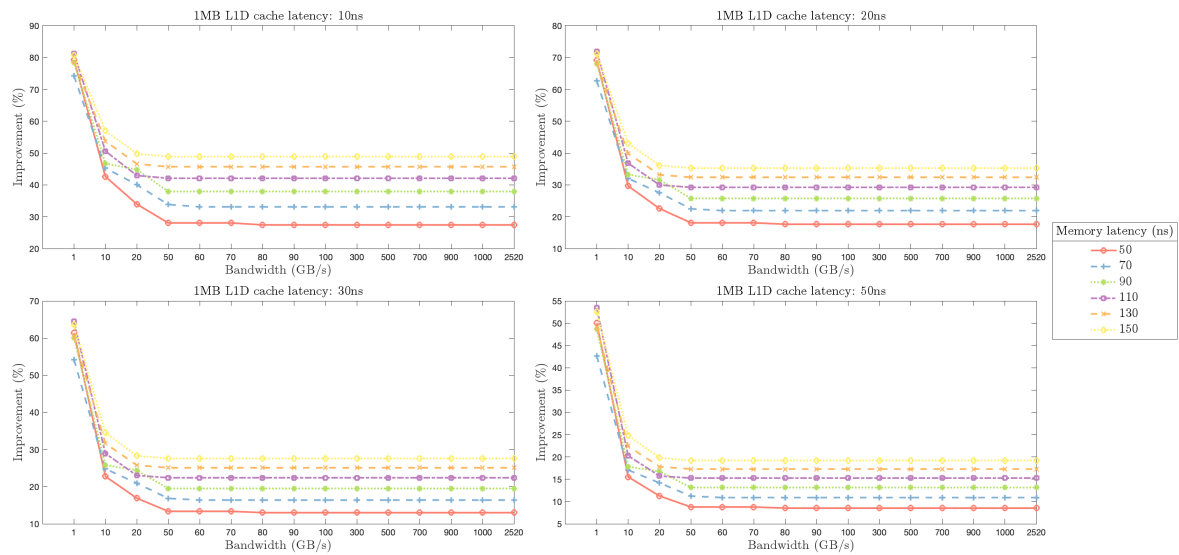


FIGURE 11: Improvement using the compressed approach compared to the non-compressed one when varying the memory bandwidth and L1 cache latency and memory latency, with a fixed 1MB cache size.

tor for other neural network workloads. Additionally, we have presented a comprehensive stack of tools designed for the development and analysis of RISC-V vectorized applications.

Our investigation included an analysis of the behavior of the bfloat16 format when utilized as a compressed format for storing image and weight data. Leveraging the seamless conversion between bfloat16 and binary32, we achieved a substantial speedup of approximately 90% compared to an uncompressed solution that uses binary32 for both storage and computations.

We believe our contribution is twofold: firstly, we have demonstrated another promising use case of reduced precision data types, specifically bfloat16; secondly, by adopting a co-design approach with simulation tools, we were able to provide valuable feedback to RTL designers, ultimately leading to improvements in the architecture and enabling the efficient utilization of compressed data type formats.

Our work exemplifies the effectiveness of the co-design approach, incorporating simulations, in obtaining early feedback crucial for the hardware design stage. This approach proves to be highly useful for optimizing and refining designs, laying the groundwork for future advancements in this domain.

REFERENCES

- [1] "RISC-V ISA Specification," <https://riscv.org/specifications/isa-spec-pdf/>, (Accessed 2020-03-11).
- [2] A. Waterman, Y. Lee, D. A. Patterson, and K. Asanovic, "The RISC-V instruction set manual, volume I: Base user-level ISA," *EECS Department, UC Berkeley, Tech. Rep. UCB/EECS-2011-62*, vol. 116, 2011.
- [3] K. Asanović and D. A. Patterson, "Instruction sets should be free: The case for RISC-V," *EECS Department, University of California, Berkeley, Tech. Rep. UCB/EECS-2014-146*, 2014.
- [4] U. Köster, T. Webb, X. Wang, M. Nassar, A. K. Bansal, W. Constable, O. Elibol, S. Gray, S. Hall, L. Hornof *et al.*, "Flexpoint: An adaptive numerical format for efficient training of deep neural networks," in *In Proc. of the 31st Conference on Neural Information Processing Systems (NIPS'17)*, 2017, pp. 1742–1752.
- [5] V. Popescu, M. Nassar, X. Wang, E. Tumer, and T. Webb, "Flexpoint: Predictive numerics for deep learning," in *In Proc. of the 25th IEEE Symposium on Computer Arithmetic (ARITH'18)*, June 2018, pp. 1–4.
- [6] N. Burgess, J. Milanovic, N. Stephens, K. Monachopoulos, and D. Mansell, "Bfloat16 processing for neural networks," in *In Proc. of the 26th IEEE Symposium on Computer Arithmetic (ARITH'19)*, 2019, pp. 88–91.
- [7] A. Agrawal, S. M. Mueller, B. M. Fleischer, X. Sun, N. Wang, J. Choi, and K. Gopalakrishnan, "Dfloat: A 16-b floating point format designed for deep learning training and inference," in *2019 IEEE 26th Symposium on Computer Arithmetic (ARITH)*, 2019, pp. 92–95.
- [8] J. Johnson, "Rethinking floating point for deep learning," *CoRR*, vol. abs/1811.01721, 2018. [Online]. Available: <http://arxiv.org/abs/1811.01721>
- [9] "Tesla Dojo Technology: A Guide to Tesla's Configurable Floating Point Formats & Arithmetic." [Online]. Available: https://tesla-cdn.thron.com/static/MXMU3S_tesla-dojo-technology_1WDVZN.pdf
- [10] J. L. Gustafson and I. T. Yonemoto, "Beating floating point at its own game: Posit arithmetic," *Supercomputing Frontiers and Innovations*, vol. 4, no. 2, pp. 71–86, 2017.
- [11] M. Cococcioni, F. Rossi, E. Ruffaldi, and S. Saponara, "Novel arithmetics to accelerate machine learning classifiers in autonomous driving applications," in *In Proc. of the 26th IEEE International Conference on Electronics, Circuits and Systems (ICECS'19)*, 2019, pp. 779–782.
- [12] M. Cococcioni, E. Ruffaldi, and S. Saponara, "Exploiting posit arithmetic for deep neural networks in autonomous driving applications," in *In Proc. of IEEE Int. Conf. of Electrical and Electronic Technologies for Automotive (Automotive'18)*, 2018, pp. 1–6.
- [13] Z. Carmichael, H. F. Langroudi, C. Khazanov, J. Lillie, J. L. Gustafson, and D. Kudithipudi, "Deep positron: A deep neural network using the posit number system," in *2019 Design, Automation*

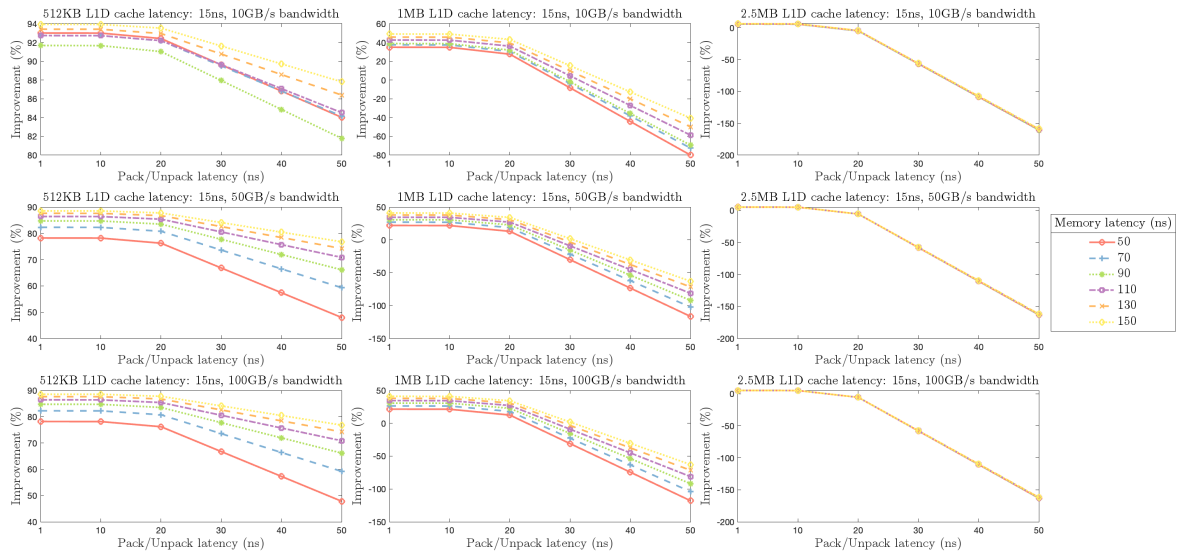


FIGURE 12: Improvement using the compressed approach when varying architectural parameters and compression/decompression instruction latency.

Test in Europe Conference Exhibition (DATE), 2019, pp. 1421–1426.

[14] S. H. Fatemi Langroudi, Z. Carmichael, J. Gustafson, and D. Kudithipudi, “Positnn framework: Tapered precision deep learning inference for the edge,” 07 2019, pp. 53–59.

[15] J. Lu, C. Fang, M. Xu, J. Lin, and Z. Wang, “Evaluations on deep neural networks training using posit number system,” *IEEE Transactions on Computers*, pp. 1–1, 2020.

[16] M. Cococcioni, F. Rossi, E. Ruffaldi, and S. Saponara, “Novel arithmetics in deep neural networks signal processing for autonomous driving: Challenges and opportunities,” *IEEE Signal Processing Magazine*, vol. 38, no. 1, pp. 97–110, 2021.

[17] —, “Small reals representations for deep learning at the edge: A comparison,” in *Next Generation Arithmetic*, J. Gustafson and V. Dimitrov, Eds. Cham: Springer International Publishing, 2022, pp. 117–133.

[18] Y. Uguen, L. Forget, and F. Dinechin, “Evaluating the hardware cost of the posit number system,” in *29th Int. Conf. on Field Programmable Logic and Applications (FPL’19)*, 2019, pp. 106–113. [Online]. Available: <https://doi.org/10.1109/FPL.2019.00026>

[19] M. Cococcioni, F. Rossi, E. Ruffaldi, and S. Saponara, “A lightweight posit processing unit for risc-v processors in deep neural network applications,” *IEEE Transactions on Emerging Topics in Computing*, vol. 10, no. 4, pp. 1898–1908, 2022.

[20] M. Cococcioni, F. Rossi, E. Ruffaldi, and S. Saponara, “Vectorizing posit operations on RISC-V for faster deep neural networks: experiments and comparison with ARM SVE,” *Neural Computing and Applications*, 2021. [Online]. Available: <https://doi.org/10.1007/s00521-021-05814-0>

[21] V. Pillet, J. Labarta, T. Cortes, and S. Girona, “Paraver: A tool to visualize and analyze parallel code,” in *Proceedings of WoTUG-18: transputer and occam developments*, vol. 44, no. 1. Citeseer, 1995, pp. 17–31.

[22] F. Mantovani and E. Calore, “Performance and power analysis of HPC workloads on heterogeneous multi-node clusters,” *Journal of Low Power Electronics and Applications*, vol. 8, no. 2, p. 13, 2018.

[23] M. Cococcioni, F. Rossi, E. Ruffaldi, and S. Saponara, “Fast approximations of activation functions in deep neural networks when using posit arithmetic,” *Sensors*, vol. 20, no. 5, 2020. [Online]. Available: <https://www.mdpi.com/1424-8220/20/5/1515>

[24] —, “A fast approximation of the hyperbolic tangent when using posit numbers and its application to deep neural networks,” *Int. Workshop on Applic. in Electronics Pervading Ind., Envir. and Society (ApplePies’19)*, 2019. [Online]. Available: http://dx.doi.org/10.1007/978-3-030-37277-4_25

[25] —, “A novel posit-based fast approximation of elu activation function for deep neural networks,” in *2020 IEEE International Conference on Smart Computing (SMARTCOMP)*, 2020, pp. 244–246.

[26] M. Cococcioni, F. Rossi, E. Ruffaldi, and S. Saponara, “Fast deep neural networks for image processing using posits and ARM scalable vector extension,” *Journal of Real-Time Image Processing*, pp. 1–13, 2020.